Enabling Localization in WSNs with Solar-Powered End Devices

Rushi Vyas, Vasileios Lakafosis, Manos Tentzeris
School of Electrical and Computer Engineering, Georgia Institute of Technology
Atlanta, Georgia, USA
Rushi.Vyas@gatech.edu

***Abstract*—A novel remote localization system utilizing renewable solar energy to power and trigger communication between end devices and a wireless network is presented. The novelty of the system is the unique node design that allows for battery less operation using ambient solar energy. Hardware and software design considerations involved in making the localization system operational inspite of the limitations of solar power are outlined. The final functioning localization system results as an end application are presented. A remote localization system with very good accuracy utilizing this end node communicating with a WSN is showcased as an end application with tremendous potential.**

Keywords- Solar; RF; Power Scavenging; WSN; localization; Ambient power; microcontroller; RFID; wireless sensor node

I. INTRODUCTION

This paper presents a fully operational localization system that tracks the position of a remotely placed end device through lateration. This service has been found to be very helpful in large parking lot environments; not only does this localization service offered help the user, for example car auction dealer, to be able to directly find any vehicle fast and accurately, but it also enables the user to exploit the location data for optimization and cost reduction of its everyday operation.

The goal of the work presented in this paper is the provision of location information of a solar powered battery-less RFID tag placed on the dashboard of a vehicle in large scale parking lots to customers, such as car auction dealers. The localization technique deployed is the RSSI (Received Signal Strength Indicator)-based lateration.

II. SYSTEM

Lateration is the method of estimating the position of an end device by using its distance from 3 or more anchor points whose exact location coordinates are known in advance. The reference points were wireless sensor network (WSN) nodes made up of Crossbow's MICA2 wireless nodes. The distance of the end device from the anchor nodes was estimated from the strength of the wireless signal transmitted from the end device as measured by Received Signal Strength Indicator (RSSI) on the TI CC1000 transceiver [2] that the MICA2 motes relied upon. RSSI measurements from the anchor node were pooled together on a central computer where they were selectively parsed for computations that would estimate the position of the end device.

The novelty of the system was that the end node not only used ambient light to power itself, but also used it as a triggering mechanism for initiating communication between itself and the WSN nodes thereby allowing for a completely stand-alone, battery-less asynchronous communication link from itself to the WSN used in the lateration [2]. The drawback of course would be that such a localization system would only be operable during day time. The elimination of the need to replace batteries every few months does makes such a system ideally suited for large scale item level tracking in many commercial applications. Section III describes the Power scavenging hardware design of the end node; Section IV describes considerations taken to establish a robust wireless communication link between the end node and WSN given the power limitations and Section V covers the wireless front end namely the amplifier characterization and antenna design of the end node; section VI describes the localization techniques used; the final results of the localization estimation using a commercial mapping software are covered in section VII.

III. HARDWARE

The hardware system for the end node that was to be remotely tracked by the WSN was designed to meet the following criteria for successful lateration: constant RF Power output during each transmission, high rate of communication, long range, omni-directionality, wireless connectivity. The fundamental problem with using a finite sized solar cell array was its scarce output power. The palm-sized solar cell array that was stacked in a parallel configuration was capable of generating a maximum of 15mW. The most power hungry portion of the end node which was the wireless front-end consumed a peak power of 48 mW in transmit mode. A comparison of the 2 numbers showed that while it was not possible to continuously power the end node with the solar cell array, in a relatively short period of time enough solar energy could be harnessed from the environment to supply the end node with just enough power for communication for a short period of time. A system level diagram of the end node is shown in Fig.1.

978-0-7695-4049-8/10 $26.00 © 2010 IEEE
DOI 10.1109/SUTC.2010.52

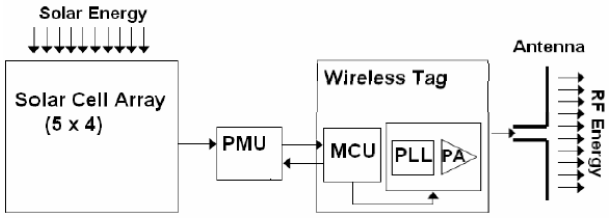

Fig. 1. System level diagram of solar powered end node. [2]

The power source of the end node comprised of an array of Solar Cells configured to give out an open circuit voltage and current above a certain minimum value under different light conditions. The Solar Cell array was interfaced to the end node through a Power Management Circuit (PMU), which was in turn interfaced to an integrated 8-bit microcontroller unit (MCU) housed in the same chip as the Wireless front-end. Communication was carried out by the wireless front-end that comprised of a single-ended Power Amp (PA) connected at its output to an appropriately designed external printed monopole antenna. The end node was made up of the following components: a palm-sized array of Solar cells, power management circuitry (PMU), an integrated 8 bit microcontroller chip (MCU), a wireless transmitter housed in the same MCU chip and an antenna [2].

A. *Solar Cell Array*

The Solar cells were arranged in an array of 5 by 4 big enough to fit in a palm sized circuit board. Each solar cell unit was a stack-up of GaAs cells with open circuit voltage node and short circuit current characteristics with respect to light intensity shown in Fig. 2. Measurements in Atlanta show light intensity to vary from 4,000 lux on a cloudy day to 60,000 lux on a clear sunny day. Light intensity measurements were performed using a LUX meter. From Fig 2, the open circuit voltage node and short circuit current of each solar cell of the PV array would vary from between 7 to 10 volts and 0-80uA based on external light conditions. The parallel configuration of the solar cells would give a maximum short circuit output current of 1.6mA while ensuring the same output voltage. Solar cells with a higher stackup that generate a higher output voltage were used based on the choice of the capacitor used in the Power Management unit. In the absence of batteries, the solar energy was to be collected in a super capacitor (charge tank) for use by the end node. [2] A higher solar cell output voltage across the capacitor would provide a faster charge-up time for different light conditions, which is important for more frequent communication by the end node as will be shown later. The drawback of using a super capacitor along with an ambient light variable power source such as a solar cell is its lack of a stable regulated voltage output when different components within the end node are powered on. A stable regulated power output is important to ensure that the RF power radiated from the end node is consistent during each transmit to the WSN to ensure accurate lateration. To rectify this, a novel Power management unit was devised that regulated the solar cell/super capacitor output to between 3 and 5.5 volts, which is the operating voltage of the end node MCU/wireless transceiver.

B. *Power Management Unit*

The Power management unit served as the interface between the solar cells and the end node. It was made up of super capacitors connected in parallel that served as the solar energy storage device. Super capacitors are much more environmentally cleaner to dispose off and offer higher recharging life times compared to batteries. Power in the form of charge stored in the capacitors was monitored by the MCU in conjunction with discrete level FET switches that were also used to switch power to the system on or off. The PMU would keep the end node in either "off" or "sleep" mode till enough of the solar energy had been collected across the charge tank capacitors. Once the capacitor voltage had reached a certain user set voltage threshold (VTH), the PMU would trigger the end node on. Once "on", the MCU of the end node would take over control of the operation of the end node [2].

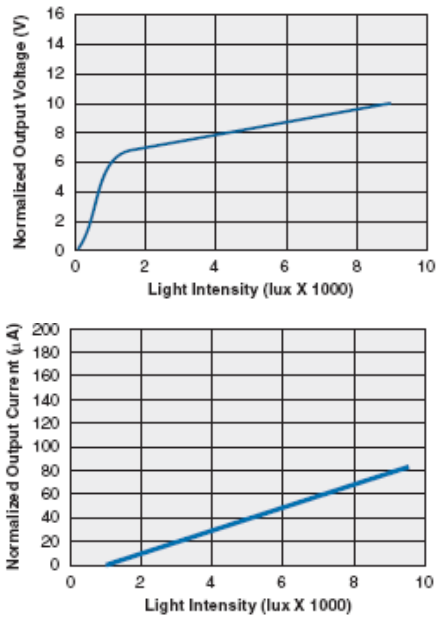

Fig. 2. Characteristic of single Solar cell used in array. [3]

The MCU firmware was designed to optimize power consumption of the end node and the MCU code was implemented to carry out data processing of the wireless data bits in as few instructions as possible to conserve power. In addition, the MCU was also programmed to power on the wireless front-end only when the end node was ready to transmit data. This was done keeping in mind that the MCU consumed only between 540 and 480 μA of current as the capacitor discharged from a threshold voltage of 3.8 to 2.2Volts, which is the voltage at which the MCU and hence the end node shuts off. On the other hand, the wireless front end along with the MCU consumed between 15.65 to 15.37mA as the charge tank discharged from the threshold voltage of 3.8 to 2.7 volts which was the voltage at which only the wireless front end unit of the end node turned off. Upon completion of

communication, the MCU would disable the wireless front end and put itself in "sleep" mode consuming micoramps of current thereby allowing the already discharged charge tank capacitor to replenish itself using solar energy and repeat the process once it got to the threshold voltage [2].

Setting a fixed voltage threshold (VTH) with the PMU ensures an identical PA output and hence an identical RF radiated power output independent of the external light conditions. The maximum available transmit time is determined by the value of the amount of solar energy harnessed or conversely the charge tank capacitance. A quick way of estimating the total transmit time (TXMIT) available for a given value of charge tank capacitance is given by eq. 1 [2].

$$T_{XMIT} = -\ln\left(\frac{V_{OFF}}{V_{TH}}\right) \times (R \times C_{TANK}) \quad (1)$$

where VOFF: Turn off Voltage of the wireless front end
VTH: Threshold voltage set in the PMU
R: Mean load resistance of the end node operating between VTH & VOFF
CTANK: Value of the charge tank capacitor

For the end node prototype developed, the threshold voltage (VTH) by the PMU was set to 3.8 volts and the end node's turn off voltage was measured to be 2.7V when transmitting using frequency shift keying (FSK) modulation around a center frequency of 904.29MHz, the mean load resistance of the end node was measured to be 194 Ω. Using eq.(1) the total transmit time was determined to be 42.23 ms for the charge tank capacitor of 637 µF used in the prototype. The approximation in eq.(1) does not take into account the power consumed in the initial processing done by the MCU, which is less than 4% of the total power consumed and the power supplied by the solar cell as the charge tank capacitor discharges. The total wireless transmit time available for a charge tank capacitance of 637uF and a PMU threshold of 3.8V in the end node is shown in the wireless signal captured by a Tektronics RSA-3408A Real Time Spectrum Analyzer (RTSA) connected to an AN-400 RFID reader antenna in the form of power vs. time in fig 3 below. The measured transmit time was observed to be 43.25ms, very close to the theoretically predicted value. The charge tank capacitance along with external light conditions would also set the time interval between adjacent transmits. Light intensity measurements carried out on the end node using a charge tank of 637uF show a linearly proportionate relationship between light intensity and the rate of wireless transmissions as can be seen from table 1. The light intensities were replicated in the lab with the help of halogen bulbs and may not represent the entire spectrum present in sunlight, therefore presenting the worst-case scenario [2]. The benefit of configuring the PMU this way was that it would work with an even smaller or less expensive solar cell array albeit at the expense of increased latency in tracking communication of the end node with the WSN nodes and hence slower tracking. Even with a solar cell array shrunken to 1/10th the size, the time interval between adjacent transmits would increase to about 44 sec i.e the end node would be tracked once every minute under less sunny conditions (10.5 kLux), which would be acceptable for many item level tracking applications including vehicles for which the proposed system was designed and tested.

IV. WIRELESS COMMUNICATION OF END NODE WITH WSN

The data packets that were transmitted by the end node to the WSN nodes within its range using FSK modulation at a center frequency of 904.3 MHz. The data packets comprised of the following fields: Preamble, Sync, Addr, Type, Group, Length, Data, and CRC. The first two fields are used for synchronization of the receiver's clock and the latter field, Cyclic Redundancy Check, helps eliminate bit errors occurring within the sent bit sequence by successfully recognizing a corrupted packet and discarding it [2].The Data bits of the packets conveyed the RFID of the end node in order to help the WSN distinguish between one or more of the end nodes. The wireless data sequence sent out by the end node as captured by the RTSA is shown in fig 4 below. The time to transmit one set of data packets was about 9ms, which given the total transmit time available for a charge tank capacitance of 637uF (transmit time of 43.23 ms) allowed for transmission of at least 4 set of data packets per energy duty cycle.

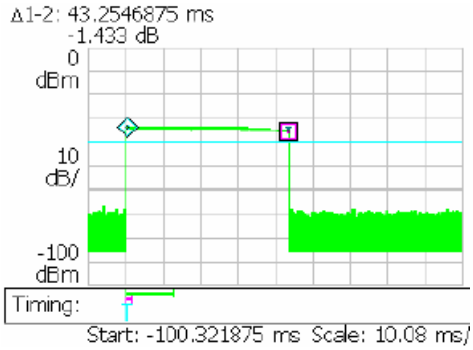

Fig. 3. Wireless transmission profile of the end node Captured by Real Time Spectrum Analyzer RTSA – Power vs. Time [2].

Table 1. Measured Rate of Wireless Transmissions.

Light Intensity Exposed on End node	*Time Interval between consecutive Wireless transmissions*
10.5 kLux	4.4 sec
20 kLux	2.7 sec
40 kLux	1.8 sec
70 kLux	1.4 sec

At the physical level, one of the ways the bit errors between the end node and the receiver was noticeably minimized was by calibrating the Phase Locked Loop (PLL) of the end node so that its modulation profile around the center frequency very closely matched to that required by the receiver MICA2 motes. This calibration also has the added advantage of requiring fewer number of preamble bits for the receiver to bit synchronize with the end node for Manchester bit encoding [4],

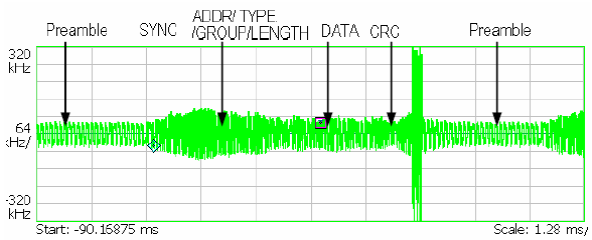

Fig. 4. Wireless data sequence (RFID) sent out by end node captured by RTSA. [2].

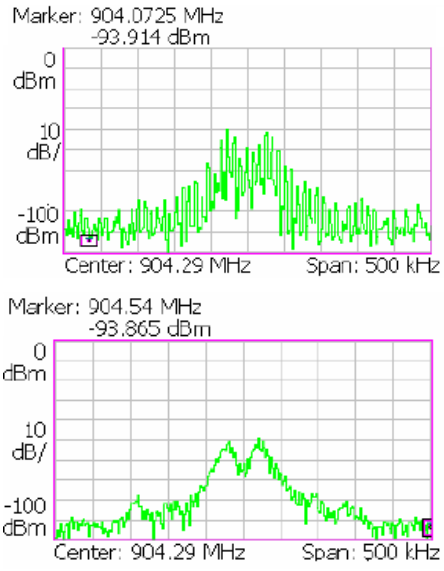

Fig. 5. Calibrated End node and Crossbow transmitter FSK modulation profile.

which given the limited amount of power available per energy duty cycle can be useful [2]. The calibrated fsk modulation profile sent by the solar powered end node and the modulation profile of a MICA2 transmitter mote designed specifically for the MICA2 mote receiver both made by Crossbow as captured by the RTSA is shown in fig 5.

V. AMPLIFIER CHARACTERIZATION AND ANTENNA DESIGN

The size of the localization area or conversely the number of WSN nodes used for the localization is a function of the range of the end node, which is dependent on a number of factors such as the gain of the antenna on the end node and wsn nodes, the maximum power transmitted by the end node and the receiver sensitivity of the receiver on the wsn nodes. The WSN nodes utilized a TI CC1000 transceiver which had a fixed sensitivity of -110 dBm matched to a 50 ohm monopole antenna [4], [5]. On the end device side, the RF power radiated should be omni-directional for an accurate localization computation. To achieve this, a customized antenna was designed for the end node. The antenna used a monopole structure to achieve a gain of 0dB that translates into omni-

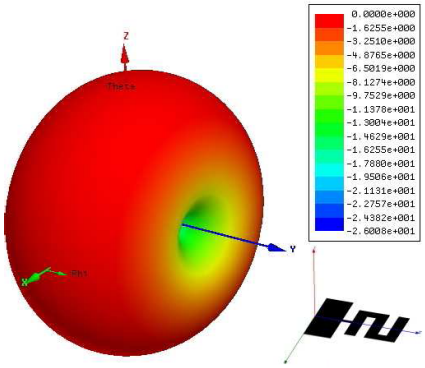

Fig. 6. Simulated end node antenna radiation pattern. [7].

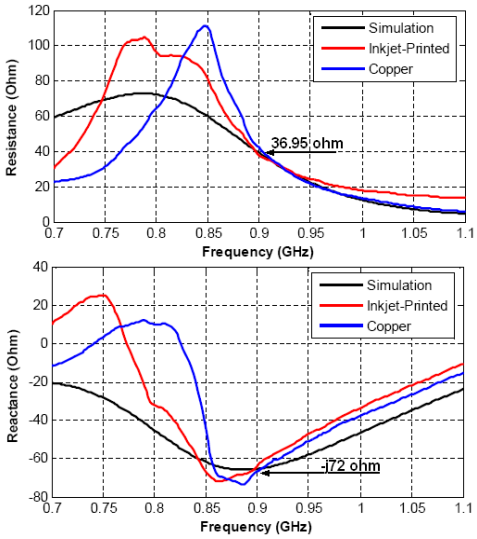

Fig. 7. Simulated and Measured end node antenna impedance [7].

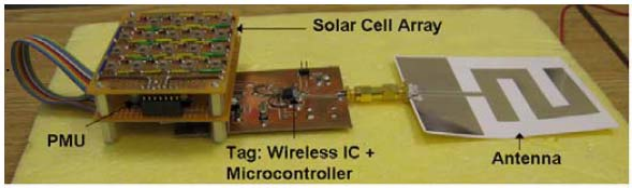

Fig. 8. Working solar powered end node prototype.

directionality [6]. In addition the antenna was tweaked to ensure that its impedance was equal to 36.95-j71.77Ω, which is the conjugate of the optimum load impedance of the amplifier in the wireless transceiver of the end node [2]. This ensures that the bulk of the solar power harnessed is radiate out from the amplifier into the Antenna as RF power. The simulated antenna radiation pattern and its measure impedance are shown in figs 6 and 7. The working prototype of the solar powered end device is shown in fig 8.

VI. LOCALIZATION

Lateration is the approach according to which distances from three (trilateration) or more (multilateration) anchor nodes, whose exact absolute location coordinates are known a priori, are used to estimate the node location. The received

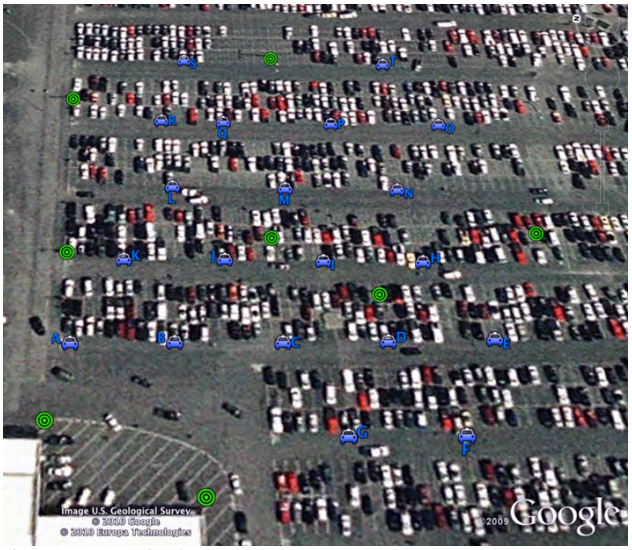

Fig. 9. WSN node placement.

signal strength indicator returned by a register of the transceiver after the successful reception of a packet from another node can serve as an estimate of physical distances. In particular, the distance from the emitter can be estimated by using this Received Signal Strength Indicator (RSSI) value along with the known effective isotropically radiated power (EIRP), which takes into account the transmission power, the antenna gain and the cables losses of the emitter, into the Friis equation. For the latter equation a particular path loss coefficient and model, which is most suitable to the actual surrounding environment, has to be chosen; in our case that was the two-ray ground reflection model [13].

The two main characteristics that render this localization method attractive are that neither additional hardware nor additional communication overhead is required. However, there are a few parameters that can degrade the accuracy of the RSSI approach. First, incorrect estimations are introduced when the RSSI is extracted from packets which have followed an indirect path due to multipath fading [11], regardless of whether they have been emitted from an anchor node in line-of- sight with the receiver or not. Second, the fast-fading effect, as well as the dynamic nature of the environment, can result in serious variations in the RSSI measurements over time. Moreover, since the widely used inexpensive radio transceivers are in most cases uncalibrated [12], the actual transmission power can differ from the configured one and the measured RSSI value might not correspond precisely to the actual received signal strength. Nevertheless, the rather painful, and for some applications impractical, process of calibrating every node in the network can entirely eliminate these latter problems. In the framework of this work, efforts to alleviate the above degrading effects have been made before the trilateration is conducted. First, rigorous mapping of the RSSI values recorded at fine grained set distances from an anchor node and for known transmit power are conducted. Additionally, in order to remove the signal noise, the RSSI data is passed through Kalman filtering [14] with the use of appropriate procedure language R functions [15].

From the radio propagation perspective, the WSN setup was carried out to allow the WSN nodes to better receive the end node transmitted data, which would result in better localization estimation. The requirement for the clearance of at least the 80% of the first Fresnel zone was satisfied [8] in most cases for the towers that were in line of sight from the vehicle's windscreen. The Mica 2 nodes that formed the WSN were mounted on lamp posts. The average height of the motes above the ground was 3.5m and the height of the end device hung from the mirror of a vehicle was around 1.5m, the value of the radius of the cross section of the ellipsoidal of the first Fresnel zone at the middle of the distance, typically 75m, was approximately 2.8m and the same value just 0.5m away from the mote side was around 0.3m.

After the successful reception from each WSN node of the beacon message transmitted by the end node, significant information, namely RSSI, unique tower id and time stamp, is appended and forwarded to a central location through an overlay 2.4GHz IEEE 802.11 wireless local area network consisting of three Linksys WRT54GL access points; one connected to the central server and the other two connected through UTP cable to each of the eight Mica motes, the ethernet interface of which was provided by an additional daughterboard. All these message entries are imported into an Sqlite database. The first type of process performed is data validity checks, according to which, a number of filters are applied to reject invalid entries due to bit errors based on their severity. Then the RSSI, after it is filtered as explained earlier, is used for the distance calculation from a particular WSN node with the use of a two-ray tracing radio propagation loss model. The timestamp information availability enables the use of a timer function, which loads data from specific time periods back in the past relative to the time the location estimate was initiated. Finally, the multilateration is performed as a database procedure calling [9] and in turn functions are called to display the returned WGS 84 latitude-longitude coordinates on Google Earth [10].

VII. LOCALIZATION ESTIMATE EVALUATION

In order to verify the feasibility of this technology for remote tracking applications, actual measurements of the location estimate error were conducted at different positions of the end device in the field, covered by a number of fixed motes. These different positions are shown in Fig. 9, whose placement resembles to an asterisk topology. The diameter of the area covered by the overall topology is around 190m and the radius of the area covered by each anchor node is roughly 90m. Examples of localization estimates returned in Google Earth and compared to their real corresponding placement are shown in Fig. 10 and 11.

The mean estimate error of all the 24 measurements was 38.56m with the maximum being 95.9m (for O) and minimum 1.62m (for G). It is worth noting that, for a subset of

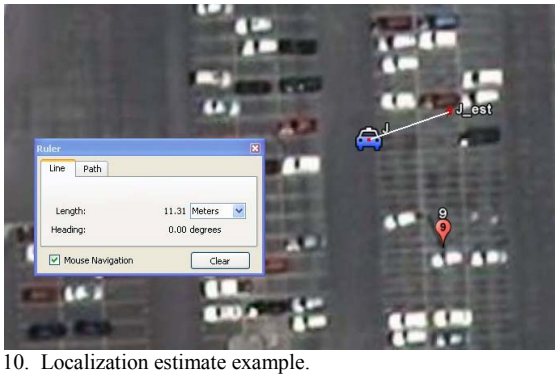

Fig. 10. Localization estimate example.

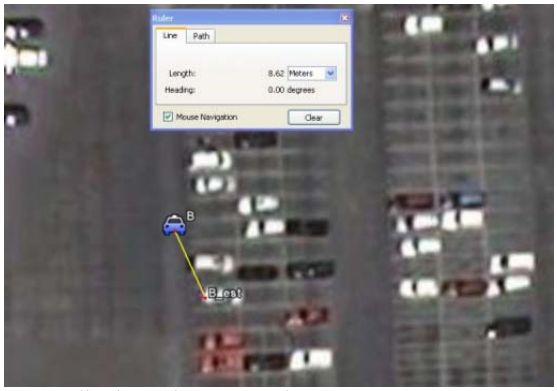

Fig.11. Localization estimate example.

measurements around the center of the topology the average error was measured to be 24.52m,. Since one of the goals of the localization experiment was to be able to locate the vicinity of a vehicle in a parking complex shown in fig 9, the average error corresponding roughly to about 3 parking spaces as can be seen from figure 10, 11 was reasonable. In contrary, the average location estimate error increased (51.98m) when the transmitter moved to the periphery or slightly outside of the virtual circular topology, where optimal coverage by multiple anchor nodes is not provided. This latter value, nevertheless, needs not been taken into consideration as the transmitter end device will always be considered to move in an area optimally wirelessly covered.

VIII. CONCLUSION

The first ever operational remote tracking system using a battery less, solar power scavenging unique node has been demonstrated. It is the first time reported that the ambient solar energy not only provides the necessary operation power of the end node being remotely located, but it also functions as the trigger of the data communication. A successful solar triggered wireless link between the end node and WSN was successfully established providing excellent localization accuracy in a sustainable way.

REFERENCES

[1] V. Lakafosis, and M.M. Tentzeris, “From Single- to Multi-hop: The Status of Wireless Localization”, Microwave Magazine, IEEE , vol.10, no.7, pp.34-41, Dec. 2009

[2] R. Vyas, V. Lakafosis, E. Tentzeris, “Design and Characterization of a Novel Battery-less, Solar Powered Wireless Tag for Enhanced Range Remote Tracking Applications” EuMW 2009, Rome, 29 September 2009

[3] Clare, “CPC 1832 Solar Cell,” Data Sheet, 2008.

[4] "CC1000 Single Chip Very Low Power RF Transceiver, Texas Instruments", 2008, [Online].

[5] MICA2 Datasheet, Crossbow [Online]. Available: http://www.xbow.com/Products/Product_pdf_files/Wireless_pdf/MICA2_Datasheet.pdf

[6] C. Balanis, Antenna Theory. New York: Wiley, 1997

[7] Konstas, Zissis, “Design and Fabrication of a Novel Conductive Inkjet Printed Antenna on Paper Substrate for RFID Applications”, Diploma thesis, Oct 2008.

[8] Les Barclay, Propagation of Radiowaves (2nd Edition), IEE, 2003, pp.123–135

[9] GTAthena Localization, Ecological Software Solutions LLC. Hegymagas, Hungary. Version 1.11

[10] Online. http://earth.google.com

[11] N. Bulusu, D. Estrin, L. Girod, and J. Heidemann, “Scalable coordination for wireless sensor networks: self-configuring localization systems”, in Proc. of the Sixth International Symposium on Communiation Theory and Applications, Ambleside, Lake District, UK, 2001

[12] K. Whitehouse, and D. Culler, “Calibration as parameter estimation in sensor networks”, in Proc. of the 1st ACM International Workshop on Sensor Networks and Applications (WSNA), Atlanta, GA, 2002.

[13] T. S. Rappaport., Wireless communications: principles and practice, Prentice Hall, ISBN-10: 0130422320, 1996.

[14] Kalman et. Al, “A New Approach to Linear Filtering & Prediction Problems” Transactions of ASME-Journal of Basic Engineering, Vol. 82D, pp.35-45, 1960.

[15] The R Project for Statistical Computing, Available: http://www.r-project.org/